The Christov-Galerkin spectral method in complex arithmetics

M. A. Christou, N. C. Papanicolaou, C. Sophocleous, and C. I. Christov

---

Articles you may be interested in

A numerical study of biofilm growth in a microgravity environment
AIP Conference Proceedings **1895**, 120001 (2017); 10.1063/1.5007418

Numerical investigation of sixth order Boussinesq equation
AIP Conference Proceedings **1895**, 110003 (2017); 10.1063/1.5007409

List of Participants: Application of Mathematics in Technical and Natural Sciences 9th International Conference - AMiTaNS'17
AIP Conference Proceedings **1895**, 130001 (2017); 10.1063/1.5007428

Method for solving the problem of nonlinear heating a cylindrical body with unknown initial temperature
AIP Conference Proceedings **1895**, 110011 (2017); 10.1063/1.5007417

High-performance computing on GPUs for resistivity logging of oil and gas wells
AIP Conference Proceedings **1895**, 120005 (2017); 10.1063/1.5007422

Preface: Application of Mathematics in Technical and Natural Sciences 9th International Conference - AMiTaNS'17
AIP Conference Proceedings **1895**, 010001 (2017); 10.1063/1.5007351

The Christov-Galerkin Spectral Method in Complex Arithmetics

M. A. Christou[1,a)], N. C. Papanicolaou[1,b)], C. Sophocleous[2,c)] and C. I. Christov[3,d)]

[1]*Department of Mathematics, University of Nicosia, 46 Makedonitissas Ave., P.O. Box 24005, CY-1700 Nicosia, Cyprus*
[2]*Department of Mathematics and Statistics, University of Cyprus, P.O. Box 20537, CY-1678 Nicosia, Cyprus*
[3]*Department of Mathematics, University of Louisiana at Lafayette, Lafayette, LA 70504, USA*

[a)]Corresponding author: christou.ma@unic.ac.cy
[b)]papanicolaou.n@unic.ac.cy
[c)]christod@ucy.ac.cy
[d)]Prof. C. I. Christov passed away prior to the submission of the manuscript.

Abstract. We apply the Christov-Galerkin spectral method for the numerical investigation of the interaction of solitons in the Cubic Nonlinear Schrödinger Equation. The issues of convergence are addressed and an algorithm is devised for the application of the method. Results are obtained for the interaction of solitons with different phase velocities and different carrier frequencies. The interactions are shown to be elastic, save for the phase shifts. The latter are extracted from the numerical solution and discussed.

INTRODUCTION

The nonlinear Schrödinger equation (NLSE) models many physical processes. Whilst the main application is in non-linear optoelectronics (propagation of optical pulses in fibers), this equation is also used as a model to problems in telecommunications, hydrodynamics, nonlinear acoustics, quantum condensates and many other nonlinear systems such as material sciences, quantum chemistry and electronics. In particular, we are interested in the $(1+1)$-dimensional Cubic Nonlinear Schrödinger Equation (CuNLSE). This equation has a prominent role in the theory of nonlinear waves, modeling propagation in Kerr media, where the nonlinearity is proportional to the intensity of the field. In nonlinear optics the CuNLSE describes the single-mode wave propagation in a fiber. These fibers allow propagation of multiple orthogonally polarized modes, which may be described by a multi-component version of the CuNLSE (see, *e.g.*, [1]). A quick look at the development of the history of soliton theory, shows that the importance of the CuNLSE is comparable with that of the Boussinesq and Korteweg-de Vries equations. If we consider more than one space dimensions, the CuNLSE is not integrable, *i.e.*, no Lax pair exists and no linear solution techniques are available. Similarly, the coupled (multi-component) system of Schrödinger equations is also non-integrable. The lack of integrability in the predominant part of practically important models motivates the development of efficient, reliable and robust numerical methods.

We are interested in physical boundary value problems in infinite domains which are pertinent to soliton theory. These are the cases when no boundary conditions are specified, but rather the square of the solution is required to be integrable on an infinite domain, that is, the solution belongs to $L^2(-\infty, \infty)$. We aim at calculating the solitary wave solutions of the CuNLSE and examining the propagation and interaction of the modulo of the solutions.

In the literature, the currently available numerical methods for studying the CuNLSE in infinite domains focus on finite difference or finite element methods, which could create several problems if one is not very careful. For example, the inevitable reduction of the infinite interval to a finite one, introduces an artificial eigenvalue problem, the latter being irrelevant to the original infinite spatial domain. Sometimes, the finite-domain problem has a solution only for some enumerable set of intervals of specific length. It can even happen that each of the finite-domain approximations only has a trivial solution, while the original problem possesses a nontrivial one, or *vice-versa*.

The difficulties which occur when using finite differences or finite elements can be overcome if we use a spectral method with a basis of localized functions which automatically satisfy the requirement that the solution belongs to $L^2(-\infty, \infty)$ space. Here we make use of the complete orthonormal (CON) system of functions proposed in [2]. The properties of this system were investigated further in [3, 4, 5]. These functions are orthogonal without weight and possess an expression for the product of two members of the system into series with respect to the system.

The relevant formulas for the functions forming the CON system can be found in [6, 7, 8], where the Galerkin technique was successfully applied to a host of equations admitting stationary propagating solutions of solitary-wave type, *e.g.*, Korteweg-de Vries (KdV), Kuramoto-Sivashinsky (KS) and Boussinesq with quadratic and cubic nonlinearities. Here, the method is developed further to the case when the sought function is complex-valued and modeled by the CuNLSE.

THE CHRISTOV-GALERKIN METHOD IN $L^2(-\infty, \infty)$

From the known spectral techniques, we choose the Galerkin method which has the advantage of simplicity in implementation in comparison with the spectral collocation method or tau-method (for other techniques, see, *e.g.*, [9, 10]). This is due to the availability of explicit formulas for the expansions of the derivatives of the basis functions into members of the CON, a property which turns out to be crucial for constructing fast and efficient numerical algorithms. Moreover, it is more accurate than pseudospectral techniques, because there is only error from the truncation of the spectral series, and no discretization error. Naturally, for a large number of terms in the spectral expansions, the Galerkin technique is less efficient than the pseudospectral one, because Fast Fourier Transforms (FFT) can be used in the latter. However, when treating physical problems, Galerkin techniques can provide a more accurate approximation since the accuracy of pseudospectral methods depends on the number of collocation points. The only issue for problems with power nonlinearities is that Galerkin techniques require explicit formulas expressing the products of members of the CON system into series with respect to the system. For instance, the Hermite functions and Laguerre functions do not possess that kind of explicit relation. The first system for which such a product formula exists was proposed in [2]. A Galerkin technique based on the said system was developed in [11, 6] and applied to the KdV and KS equations with quadratic nonlinearity. The same technique was also employed to numerically investigate problems with cubic nonlinearity [7]. In a sequence of papers [3, 12], Boyd described a general method of constructing CON systems in $L^2(-\infty, \infty)$ by means of coordinate transformations to a finite interval and use of Chebyshev polynomials (see [9]).

The CON system we use in the present work was established by Christov [2] as the real and imaginary parts of the Wiener functions

$$\rho_n = \frac{1}{\sqrt{\pi}} \frac{(ix-1)^n}{(ix+1)^{n+1}}, \quad n = 0, 1, 2, ... \tag{1}$$

which were introduced by Wiener (see [13]), as Fourier transforms of the Laguerre functions (functions of parabolic cylinder). Higgins [14] extended it to negative indices n and proved its completeness and orthogonality. The significance of Eq. (1) for nonlinear problems was demonstrated in [2], where the product formula was derived and the two real-valued subsequences of odd functions S_n and even functions C_n were introduced, namely,

$$\rho_n \rho_k = \frac{\rho_{n+k} - \rho_{n-k}}{2\sqrt{\pi}}, \qquad S_n = \frac{\rho_n + \rho_{-n-1}}{i\sqrt{2}}, \quad C_n = \frac{\rho_n - \rho_{-n-1}}{\sqrt{2}}. \tag{2}$$

In [6], representation (3) for functions $C_n(x)$ and $S_n(x)$ was demonstrated, showing their connection with the Fourier functions $\sin x$ and $\cos x$,

$$C_n(x) = (-1)^n \frac{\cos(n+1)\theta + \cos n\theta}{\sqrt{2}}, \quad S_n(x) = (-1)^{n+1} \frac{\sin(n+1)\theta + \sin n\theta}{\sqrt{2}}, \tag{3}$$

where $x = \tan(\frac{\theta}{2})$ is the transformation of the independent variable. The importance of the connection to the periodic functions was discussed in [4].

From [2] we obtain the double product formulas of C_n and S_n expressed in series with reference to the system,

namely,

$$C_n C_k = \frac{1}{\sqrt{2\pi}} \left[\ C_{n+k+1} - C_{n+k} - C_{n-k} + C_{n-k-1} \right] , \tag{4}$$

$$S_n S_k = \frac{1}{\sqrt{2\pi}} \left[\ C_{n+k+1} - C_{n+k} + C_{n-k} - C_{n-k-1} \right] , \tag{5}$$

$$S_n C_k = \frac{1}{\sqrt{2\pi}} \left[-S_{n+k+1} + S_{n+k} + S_{n-k} - S_{n-k-1} \right] . \tag{6}$$

Now, if we make use of Eqs. (2), (4), (5) and (6) one easily shows that the triple products of members are expanded in series with respect to the system as follows (see [7]),

$$C_l C_n C_k \overset{\text{def}}{=} \sum_{m=0}^{\infty} \beta_{lnk,m} C_m(x) , \qquad\qquad \beta_{lnk,m} = \delta_{m,n+k+l+2} - 2\delta_{m,n+k+l+1} + \delta_{m,n+k+l} \tag{7}$$

$$
\begin{aligned}
&- 2\text{sgn}(l-n-k-0.5)\,\delta_{m,[|l-n-k-0.5|]} - 2\text{sgn}(l-n+k-0.5)\,\delta_{m,[|l-n+k-0.5|]} - 2\text{sgn}(l+n-k-0.5)\,\delta_{m,[|l+n-k-0.5|]} \\
&+ \ \text{sgn}(l-n-k-1.5)\,\delta_{m,[|l-n-k-1.5|]} + \ \text{sgn}(l-n-k+0.5)\,\delta_{m,[|l-n-k+0.5|]} + 2\text{sgn}(l+n-k+0.5)\,\delta_{m,[|l+n-k+0.5|]} \\
&+ 2\text{sgn}(l-n+k+0.5)\,\delta_{m,[|l-n+k+0.5|]} - \ \text{sgn}(l+n-k+1.5)\,\delta_{m,[|l+n-k+1.5|]} - \ \text{sgn}(l-n+k+1.5)\,\delta_{m,[|l-n+k+1.5|]} ,
\end{aligned}
$$

where $[a]$ stands for the largest integer number smaller than a and δ is the Kronecker delta-function. In like fashion,

$$S_l S_n S_k \overset{\text{def}}{=} \sum_{m=0}^{\infty} \alpha_{lnk,m} S_m(x) , \qquad\qquad \alpha_{lnk,m} = -\delta_{m,n+k+l+2} + 2\delta_{m,n+k+l+1} - \delta_{m,n+k+l} \tag{8}$$

$$
\begin{aligned}
&+ 2\delta_{m,[|l-n-k-0.5|]} - \ \delta_{m,[|l-n+k-0.5|]} - \ \delta_{m,[|l+n-k-0.5|]} - \ \delta_{m,[|l-n-k-1.5|]} - \ \delta_{m,[|l-n-k+0.5|]} \\
&+ 2\delta_{m,[|l+n-k+0.5|]} + 2\delta_{m,[|l-n+k+0.5|]} - \ \delta_{m,[|l+n-k+1.5|]} - \ \delta_{m,[|l-n+k+1.5|]} ,
\end{aligned}
$$

$$S_l S_n C_k \overset{\text{def}}{=} \sum_{m=0}^{\infty} \bar{\gamma}_{lnk,m} C_m(x) , \qquad\qquad \bar{\gamma}_{lnk,m} = -\delta_{m,n+k+l+2} + 2\delta_{m,n+k+l+1} - \delta_{m,n+k+l} \tag{9}$$

$$
\begin{aligned}
&- 2\text{sgn}(l-n-k-0.5)\,\delta_{m,[|l-n-k-0.5|]} - \ \text{sgn}(l-n+k-0.5)\,\delta_{m,[|l-n+k-0.5|]} + \ \text{sgn}(l+n-k-0.5)\,\delta_{m,[|l+n-k-0.5|]} \\
&+ \ \text{sgn}(l-n-k-1.5)\,\delta_{m,[|l-n-k-1.5|]} + \ \text{sgn}(l-n-k+0.5)\,\delta_{m,[|l-n-k+0.5|]} - 2\text{sgn}(l+n-k+0.5)\,\delta_{m,[|l+n-k+0.5|]} \\
&+ 2\text{sgn}(l-n+k+0.5)\,\delta_{m,[|l-n+k+0.5|]} + \ \text{sgn}(l+n-k+1.5)\,\delta_{m,[|l+n-k+1.5|]} - \ \text{sgn}(l-n+k+1.5)\,\delta_{m,[|l-n+k+1.5|]} ,
\end{aligned}
$$

$$S_l C_n C_k \overset{\text{def}}{=} \sum_{m=0}^{\infty} \bar{\bar{\gamma}}_{lnk,m} S_m(x) , \qquad\qquad \bar{\bar{\gamma}}_{lnk,m} = -\delta_{m,n+k+l+2} + 2\delta_{m,n+k+l+1} - \delta_{m,n+k+l} \tag{10}$$

$$
\begin{aligned}
&+ 2\delta_{m,[|l-n-k-0.5|]} + \ \delta_{m,[|l-n+k-0.5|]} + \ \delta_{m,[|l+n-k-0.5|]} - \ \delta_{m,[|l-n-k-1.5|]} - \ \delta_{m,[|l-n-k+0.5|]} \\
&- 2\delta_{m,[|l+n-k+0.5|]} - 2\delta_{m,[|l-n+k+0.5|]} + \ \delta_{m,[|l+n-k+1.5|]} + \ \delta_{m,[|l-n+k+1.5|]} .
\end{aligned}
$$

For the second derivative of the basis functions one has (see [2])

$$C_n'' = \sum_{m=0}^{\infty} \chi_{m,n} C_m , \qquad S_n'' = \sum_{m=0}^{\infty} \chi_{m,n} S_m , \tag{11}$$

$$\chi_{m,n} = -\frac{1}{4}n(n-1)\delta_{m,n-2} + n^2\delta_{m,n-1} - \frac{1}{4}(n+1)(n+2)\delta_{m,n+2} - \frac{1}{4}n^2 + (2n+1)^2 + (n+1)^2\delta_{m,n} + (n+1)^2\delta_{m,n+1}. \tag{12}$$

It is important to note that the matrices representing the derivatives of the basis functions in spectral space are multidiagonal, further enhancing the computational efficiency of the developed here technique. The positive definiteness of matrix χ_{nm} and the bounds on its eigenvalues were shown in [4]. These properties are essential for constructing the implicit scheme employed here.

A very important characteristic of a spectral method is its rate of convergence. Since there is a connection with the Fourier functions (see Eq. (3)), which are known to have exponential convergence, we can infer the exponential

convergence of the spectral series for the functions C_n and S_n. In [9], a detailed discussion can be found about the actual convergence rate, which while still being exponential, may turn out to be sub-geometric. Extending the arguments from [9], one expects sub-geometric convergence because of the fact that the CON system has algebraic decay at infinity, while the actual behavior at infinity of the sought solution may be different. This creates a subtle mismatch between the behaviors of the CON system and the solution that can result in a slower convergence rate. Nonetheless, the important claim here is that the convergence is exponential because even sub-geometric convergence is fast enough for most practical purposes. As it is shown in what follows, the convergence rate for the solitons considered here is actually geometric.

POSING THE PROBLEM

In what follows we focus on the CuNLS equation with a linear potential term namely,

$$i u_t + u_{xx} + |u|^2 u + \kappa u = 0, \tag{13}$$

and we use $\kappa = 1$ in actual numerical computations. Guided by the way an analytic steady solution is found for the NLS without the linear potential, we seek a soliton solution of CuNLS in the form of an envelop solution

$$u(x, t) = A e^{i\theta} \exp\left[i\left(\frac{1}{2}c(x - ct) + \eta t\right)\right] \text{sech}[a(x - ct)], \tag{14}$$

where A and a are unknown. The phase speed c, the carrier frequency η of the underlying wave, and the phase θ are prescribed in advance. Upon introducing the last expression in Eq. (13) we render the latter to

$$A\left(\frac{1}{4}c^2 - \eta + a^2 + \kappa\right) \text{sech}[a(x - ct)] + (A^3 - 2Aa)\text{sech}^3[a(x - ct)] = 0. \tag{15}$$

This equation is satisfied for

$$a = \sqrt{\eta - \frac{1}{4}c^2 - \kappa}, \quad A = \pm \sqrt{2}a. \tag{16}$$

We seek a solitary-wave solution of Eq. (13) which approaches zero as $x \to \pm\infty$ and hence all its derivatives decay automatically at zero. When treating the problem analytically one may also impose asymptotic boundary conditions on the second, third, *etc.* derivative. These are corollaries from the original b.c and are called asymptotic boundary conditions (*a.b.c.*), namely

$$u(x, t) = u'(x, t) = \ldots \to 0, \quad \text{for} \quad x \to \pm\infty. \tag{17}$$

We also mention that re-scaling the spatial variable x does not change the nature of the asymptotic boundary value problem in $L^2(-\infty, +\infty)$. Upon introducing $z = \zeta x$ we recast (13) as

$$i u_t + \zeta^{-2} u_{zz} + |u|^2 u + \kappa u = 0 \quad \text{with a.b.c} \quad u(z, t) \to 0, \quad \text{for} \quad z \to \pm\infty. \tag{18}$$

The scaling parameter ζ can be used to optimize the method in the sense that its introduction allows one to bring in concert the typical length scales of the employed system of functions in accordance with the support of the sought localized solution. Naturally, such a coordination between the scales will result in a faster convergence rate of the Fourier-Galerkin series.

For the time-dependent problem we use as initial condition the superposition of two analytical solutions of type Eq. (14), each of them with its own intrinsic parameters c_i, η_i, θ_i ($i = 1, 2$). Based on formulas Eq. (16), the respective values of a_i are calculated. We consider the two *sech*-es at positions X_i, and $|X_1 - X_2| \gg 1$, so that they do not interact at the initial moment of time $t = 0$. If this is the case, a mere superposition of two one-soliton solutions approximates the respective two-soliton solution very well. Thus,

$$u_0(z, t) = \sqrt{2a_1} \exp\left[i\left(\frac{1}{2}c_1(z/\zeta - c_1 t) + \eta_1 t + \theta_1\right)\right] \times \text{sech}\left[a\left(\frac{z}{\zeta} - X_1 - c_1 t\right)\right]$$

$$+ \sqrt{2a_2} \exp\left[i\left(\frac{1}{2}c_2(z/\zeta - c_2 t) + \eta_2 t + \theta_2\right)\right] \times \text{sech}\left[a\left(\frac{z}{\zeta} - X_2 - c_2 t\right)\right]. \tag{19}$$

SPECTRAL EXPANSION AND ALGORITHM

For the solution of system (18) we choose a semi-implicit time-stepping scheme of Crank-Nicolson type for the linear terms and explicit approximations for the nonlinear term,

$$\mathrm{i}\,\frac{u^{n+1}-u^n}{\tau} + \frac{\zeta^2}{2}[u^{n+1}_{zz} + u^{n-1}_{zz}] + u^n|u^n|^2 + \frac{\kappa}{2}[u^{n+1} + u^{n-1}] = 0, \tag{20}$$

where $t^n = t + n\tau$ and τ is the time increment. We develop the sought solution u into series with respect to the subsequences C_n and S_n, namely,

$$u^n(z) = \sum_{n=0}^{\infty} a^n_m C_m(z) + b^n_m S_m(z), \tag{21}$$

where the coefficients a_m and b_m are complex. Then, for the coefficients of the even and odd functions we have respectively

$$\begin{aligned}
\mathrm{i}\frac{a^{l+1}_m - a^l_m}{\tau} &+ \frac{\zeta^2}{2}\sum_{k=0}^{\infty}\left(a^{l+1}_k + a^{l-1}_k\right)\chi_{m,k} + \frac{\kappa}{2}\left(a^{l+1}_m + a^{l-1}_m\right) = -\sum_{k_1=0}^{\infty}\sum_{k_2=0}^{\infty}\sum_{k_3=0}^{\infty}\left(a^l_{k_1}|a^l_{k_2}||a^l_{k_3}|\beta_{k_1 k_2 k_3,m}\right. \\
&+ a^l_{k_1}|b^l_{k_2}||b^l_{k_3}|\bar{\gamma}_{k_1 k_2 k_3,m} + 2b^l_{k_1}\left(\mathrm{Re}(a^l_{k_2})\mathrm{Re}(b^l_{k_3}) + \mathrm{Im}(a^l_{k_2})\mathrm{Im}(b^l_{k_3})\right)\bar{\gamma}_{k_1 k_2 k_3,m}\Bigg)
\end{aligned}$$

$$\begin{aligned}
\mathrm{i}\frac{b^{l+1}_m - b^l_m}{\tau} &+ \frac{\zeta^2}{2}\sum_{k=0}^{\infty}\left(b^{l+1}_k + b^{l-1}_k\right)\chi_{m,k} + \frac{\kappa}{2}\left(b^{l+1}_m + b^{l-1}_m\right) = -\sum_{k_1=0}^{\infty}\sum_{k_2=0}^{\infty}\sum_{k_3=0}^{\infty}\left(b^l_{k_1}|b^l_{k_2}||b^l_{k_3}|\alpha_{k_1 k_2 k_3,m}\right. \\
&+ b^l_{k_1}|a^l_{k_2}||a^l_{k_3}|\bar{\bar{\gamma}}_{k_1 k_2 k_3,m} + 2b^l_{k_1}\left(\mathrm{Re}(a^l_{k_2})\mathrm{Re}(b^l_{k_3}) + \mathrm{Im}(a^l_{k_2})\mathrm{Im}(b^l_{k_3})\right)\bar{\bar{\gamma}}_{k_1 k_2 k_3,m}\Bigg).
\end{aligned} \tag{22}$$

In the above formulas, β, α, $\bar{\gamma}$, and $\bar{\bar{\gamma}}$ are given in Eqs. (7), (8), (9), and (10), respectively. In the numerical calculations we truncate the above systems to, say N, which means that we solve in each case $N + 1$ equations for the $N + 1$ unknowns $C_0, C_1, \ldots, C_N$ or $S_0, S_1, \ldots, S_N$, respectively.

The initial conditions for the Fourier-Galerkin coefficients $\{a^0_n\}$, $\{b^0_n\}$ and $\{a^1_n\}$, $\{b^1_n\}$ are calculated for $t = 0$ and $t = \tau$ by means of numerical quadrature of the analytical formulas after multiplying them by C_n or S_n and using numerical quadratures to obtain the coefficients of the Fourier-Galerkin series. For the inversion of the pentadiagonal matrix, we used an algorithm based on Gaussian elimination with pivoting developed in [15].

CONVERGENCE AND VALIDATION OF ALGORITHM

As we have already mentioned, the convergence rate of the Galerkin series with the chosen here CON system is exponential. It is important to verify that we actually obtain this convergence rate numerically. We explore this property of the CON systems by taking a close look at the way a superposition of two solitons is expanded into series. As featuring examples we take two cases. The first case is of two equal solitons with phase speeds $c_1 = -c_2 = 2.5$ situated relatively far from each other, $X_1 = -10, X_2 = 10$. The second case involves two nonequal solitons with phase speeds $c_1 = 2.5$, $c_2 = -1.0$ situated closer at $X_1 = -6, X_2 = 6$. The respective profiles of the superposition of the solitons are expanded into the CON system using numerical quadratures with $100,000$ grid points. This ensures that the truncation error of the numerical quadrature is negligible. The number of points is more important here than in the case of *sech* solitons, because now the profiles are oscillatory pulses whose envelope is the smooth function *sech*.

Figure 1 presents the behavior of the coefficients for the real and imaginary parts of the initial condition for the first of the above described cases. The absolute values of the computed even coefficients and the best-fitting exponential functions are plotted for three different values of the scale ζ. Table 1 gives the numerical values of best-fit exponents for different ζ's. The important observation is that the convergence is not just exponential, but is actually geometric. It is clearly seen that there is an optimum at $\zeta = 0.2$ for which value the convergence is faster (the most negative exponent of the best-fit line). The optimal value of ζ is connected with the distance between the two pulses, because when the latter are situated farther from each other, the characteristic length of the superposition is larger. Since ζ is related to the inverse of the characteristic length, a larger distance between the pulses entails smaller ζ. This is demonstrated in Figure 2 and in Table 2 where the results for the second case (the tighter initial configuration)
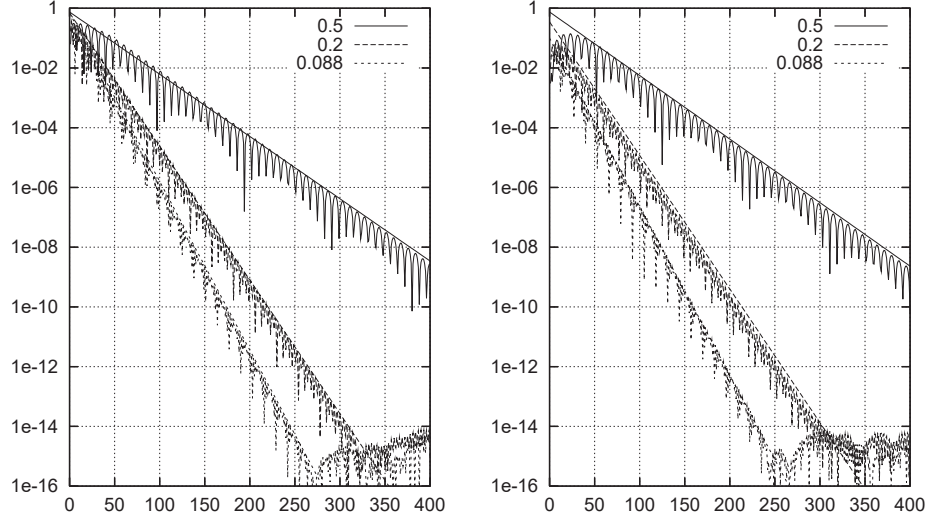
FIGURE 1. Decay rate of the Galerkin coefficients for $c_1 = -c_2 = 2.5$ and $X_1 = -10, X_2 = 10$. Left panel: real part. Right panel: imaginary part

TABLE 1. Best-fit formulas for the exponential convergence rate.

ζ	Even Coefficients for $p(x,t)$ (left panel of Figure 1)	Even Coefficients for $r(x,t)$ (right panel of Figure 1)
0.5	$0.75 \exp(-0.048n)$	$0.75 \exp(-0.049n)$
0.2	$0.7 \exp(-0.103n)$	$0.35 \exp(-0.103n)$
0.088	$0.7 \exp(-0.13n)$	$0.088 \exp(-0.13n)$
0.07	$0.7 \exp(-0.125n)$	$0.1 \exp(-0.122n)$

TABLE 2. Best-fit formulas for the exponential convergence rate.

ζ	Even Coefficients for $p(x,t)$ (left panel of Figure 2)	Even Coefficients for $r(x,t)$ (right panel of Figure 2)
0.7	$0.75 \exp(-0.07n)$	$0.75 \exp(-0.068n)$
0.5	$0.7 \exp(-0.093n)$	$0.7 \exp(-0.091n)$
0.2	$0.7 \exp(-0.16n)$	$0.7 \exp(-0.155n)$
0.1	$0.25 \exp(-0.14n)$	$0.1 \exp(-0.136n)$

are showed. Clearly, the tighter initial configuration (smaller support of the superposition) requires larger ζ for best convergence.

Note that the results presented in Figures s1, 2 are scaled by the maximal values of the respective coefficients, the best-fit curves have different amplitudes. Similar results and comparisons were obtained and made and for the coefficients of the odd functions of the system. The findings are the same as for the even coefficients.

In this paper, we consider systems of solitons that are well separated (in order not to overlap significantly), but that are not very far from each other in order not to loose the localization). In each particular case the investigation begins with choosing the optimal ζ. After extensive numerical experiments we found that for $X_2 - X_1 = 20$ the optimal value for the scaling parameter is in the interval $\zeta \in [0.1, 0.3]$ and for the case $X_2 - X_1 = 12$, the optimal interval is $\zeta \in [0.4, 0.6]$. Since in the initial moments the solitons are separated by the largest distance, we can use the initial profile to tune the parameters of the method before starting the actual calculations.
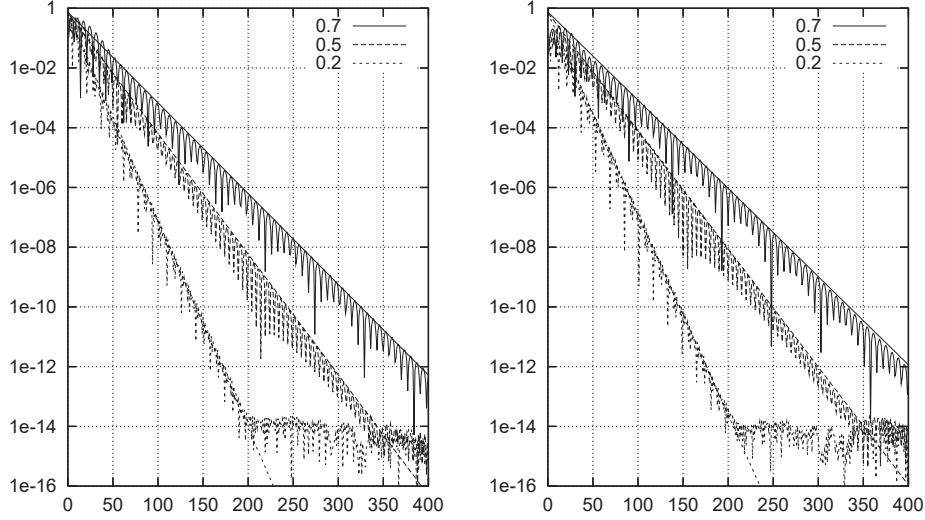
FIGURE 2. Decay rate of the Galerkin coefficients for $c_1 = 2.5$, $c_2 = -1.0$ and $X_1 = -6$, $X_2 = 6$. Left panel: real part. Right panel: imaginary part

RESULTS AND DISCUSSION

As was already mentioned in a previous section, the amplitude of the localized wave, for both the real and imaginary parts, is $A = \sqrt{2}a = \pm\sqrt{2(\eta - \frac{1}{4}c^2 - \kappa)}$. We examined several cases for different values of the parameters η and c. For the purposes of the current work, we fixed η and varied the phase speed c. We only consider localized waves with positive amplitude because the minus sign merely corresponds to a change in the initial phase.

Before proceeding to the presentation of the results, we mention here that an extensive set of numerical experiments has been conducted in order to outline the interval for the time increment τ in which the spectral solution has a satisfactory approximation and is stable. Because of the strongly implicit character of the scheme we were able to use very large time steps up to $\tau = 0.1$, but chose in most cases $\tau < 0.01$ based on considerations for better approximation of the time-dependent problem.

The next important question is whether coefficients behave well as functions of time. Due to the inevitable round-off errors, after thousands of time steps, one can expect accumulation of error, especially in the coefficients with large numbers whose values are quite close to the round-off error limit. Our calculations show that the round-off error never spreads up the spectrum to coefficients that are larger than 10^{-5}. In fact, when the total number of coefficients, N is large enough, the round-off error does not spread to coefficients that are larger than 10^{-7}. This means that the error introduced in the calculated function is practically undetectable.

Generally speaking, it is possible that for larger times, the round-off error can spread to coefficients with smaller numbers, but then the solitons will be so far from each other that the very concept of approximating them with localized functions will become questionable. This means that for the time intervals of interest (when the solitons still interact with each other), the Galerkin technique proposed here is fully adequate. Indeed, no visible distortion of the wave profiles is observed in Figure 3 for the case of two equal phase speeds $c_1 = -c_2 = 1$. Smaller phase speeds mean larger-amplitude solitons, hence for this case the nonlinearity is much more pronounced compared to the previously considered $c_1 = -c_2 = 2.5$. The results show that even here, the technique performs very well.

As another featuring example, we consider solitons with different phase speeds: $c_1 = 3$ and $c_2 = -1$ (see Figure 4).

In all of the above presented cases, the shapes and the energies of the solitons are preserved with high order of accuracy upon their collisions. Note that even the slightest but persistent "leakage" of energy during the calculations would have led to eventual linear dispersion of the solution and disappearance of the permanent shapes.

Finally, we focus our attention on the phase shift experienced during the interaction of two or more solitons. The phase shift experienced by a soliton during the collision with another one, is the difference in the actual position of the soliton and the position it would have had reached if no other solitons were present. To further investigate the issues connected with the phase shifts, we conducted a number of numerical experiments and obtained results for the phase
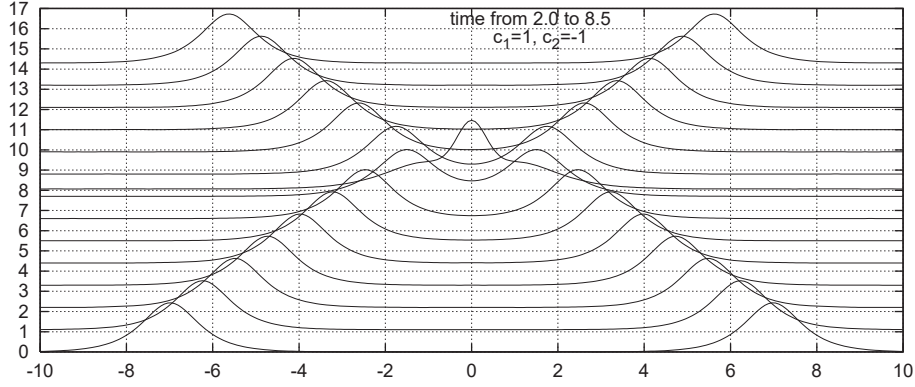
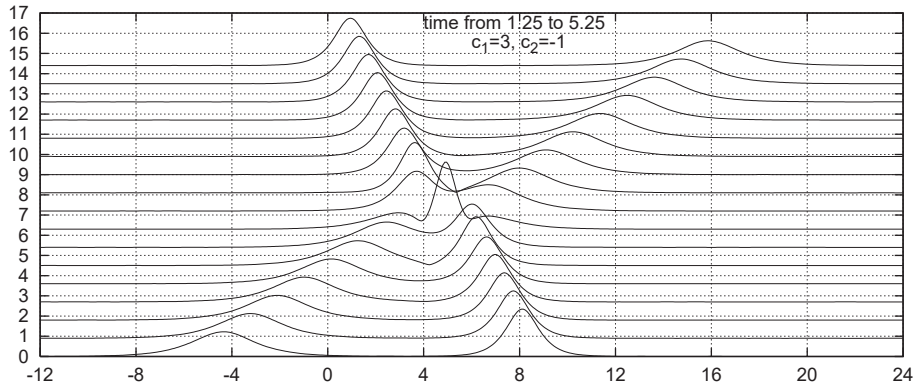**FIGURE 3.** Interaction of solitons for $c_1 = -c_2 = 1$

FIGURE 4. Interaction of solitons for $c_1 = 3$ and $c_2 = 1$

shifts for different initial configurations of the solitons. A selection of phase shifts is presented in Tables 3. In the first four columns we present the phase shifts obtained for solitons with the same initial carrier frequencies, η_i. The case with different carrier frequencies is presented in the last four columns of the table.

TABLE 3. Numerically identified phase shifts δ_i

$\eta_1 = \eta_2 = 2.0$				$\eta_1 = 2.0, \eta_2 = 3.0$			
c_1	δ_1	c_2	δ_2	c_1	δ_1	c_2	δ_2
1.95	3.92	-0.65	3.2	3.2	2.4	-2.0	0.89
0.65	4.64	-0.65	4.64	3.2	3.36	-3.2	1.84
1.95	3.76	-1.95	3.76	2.0	3.04	-2.0	2.56

The qualitative behavior of the phase shifts is in agreement with the other soliton models, such as Boussinesq and Korteweg-de Vries equations, namely the larger soliton experiences a smaller phase shift after the interaction. Indeed, we see from the table that the solitons with smaller phase shifts (i.e., with larger amplitude) are shifted less. An interesting observation here is related to the role of the carrier frequency. As we can see from the second part of the table, increasing the value of the carrier frequency decreases the magnitude of the phase shift experienced by the respective soliton with all other conditions kept the same.

It is important to note that the accurate representation of the phase shifts demonstrates that in the framework of the spectral approximation of the spatial terms, the second-order approximation in time produces almost insignificant phase error. Note that this is not the case with finite difference approximations where the temporal approximation results in somewhat larger phase error.

CONCLUSIONS

The Christov-Galerkin spectral technique was extended to complex arithmetics. A numerical scheme implementing the technique was developed and used to investigate the time-dependent problem of soliton interactions for the Cubic Nonlinear Schrödinger Equation. It was found that the computed shapes and energies of the solitons were preserved with high-order accuracy upon their collisions. Futhermore, the convergence rate of the spectral series was found to be geometric. The current results suggest the application of the method to the cubic-quintic nonlinear Schrödinger equation, which models many problems of physical interest.

ACKNOWLEDGEMENTS

REFERENCES

[1]   C. Sophocleous and D. F. Parker (1994) *Optics Communications* **112**, 214–224.
[2]   C. I. Christov (1982) *SIAM J. Appl. Math.* **42**, 1337–1344.
[3]   J. P. Boyd (1990), *J. Approx. Theory* **61**, 98–105.
[4]   J. A. C. Weidemann (1992) *Numer. Math.* **61**, 409–431.
[5]   E. I. Moiseev and A. P. Prudnikov (1993) *J. Comp. Applied. Math.* **49**, 201–206.
[6]   C. I. Christov and K. L. Bekyarov (1990) *SIAM J. Sci. Stat. Comp.* **11**, 631–647.
[7]   M. A. Christou and C. I. Christov (2002) *J. Computat. Anal. Appl.* **4,** 63–77.
[8]   M. A. Christou and C. I. Christov (2002) *J. Neural Parallel Sci. Computations* **10**, 431–447.
[9]   J. P. Boyd, *Chebyshev and Fourier Spectral Methods*, 2nd edn (Dover, New York, 2001).
[10]   C. Canuto, M. Y. Hussaini, A. Quarteroni, and T. A. Zang, *Spectral Methods in Fluid Dynamics* (SpringerVerlag, New York, 1988).
[11]   C. I. Christov (1982/87) *Ann. Univ. Sof., Fac. Math. Mech.* **76**, 87–113.
[12]   J. P. Boyd (1987) *J. Comp. Phys.* **69**, 112–142.
[13]   N.Wiener, *Extrapolation, Interpolation and Smoothing of Stationary Time Series* (Technology Press MIT and John Wiley, New York, 1949).
[14]   J. R. Higgins, *Completeness and Basis Properties of Sets of Special Functions* (Cambridge University Press, London, 1977).
[15]   M. D. Todorov and C. I. Christov, *Discr. Cont. Dyn. Syst.* Suppl. 2007, 982–992.